Intravoxel incoherent motion as a tool to detect early microstructural changes in meningiomas treated with proton therapy

Andrea Franconeri [1,3,8] · Simone Sacco [2,3] · Maria Vittoria Raciti [1,3,8] · Alessia Maggi [1,3,8] · Shaun Ivan Muzic [1,8] · Sara Imparato [3] · Lisa Farina [3,4] · Ana Bacila [3,4] · Chiara Paganelli [5,6] · Giulia Buizza [5,6] · Giulia Fontana [6] · Guido Baroni [5,6] · Giulia Riva [7] · Alberto Iannalfi [7] · Ester Orlandi [7] · Lorenzo Preda [1,3,8]

Abstract

Purpose To assess early microstructural changes of meningiomas treated with proton therapy through quantitative analysis of intravoxel incoherent motion (IVIM) and diffusion-weighted imaging (DWI) parameters.

Methods Seventeen subjects with meningiomas that were eligible for proton therapy treatment were retrospectively enrolled. Each subject underwent a magnetic resonance imaging (MRI) including DWI sequences and IVIM assessments at baseline, immediately before the 1st (t0), 10th (t10), 20th (t20), and 30th (t30) treatment fraction and at follow-up. Manual tumor contours were drawn on T2-weighted images by two expert neuroradiologists and then rigidly registered to DWI images. Median values of the apparent diffusion coefficient (ADC), true diffusion (D), pseudo-diffusion (D*), and perfusion fraction (f) were extracted at all timepoints. Statistical analysis was performed using the pairwise Wilcoxon test.

Results Statistically significant differences from baseline to follow-up were found for ADC, D, and D* values, with a progressive increase in ADC and D in conjunction with a progressive decrease in D*. MRI during treatment showed statistically significant differences in D values between t0 and t20 ($p = 0.03$) and t0 and t30 ($p = 0.02$), and for ADC values between t0 and t20 ($p = 0.04$), t10 and t20 ($p = 0.02$), and t10 and t30 ($p = 0.035$). Subjects that showed a volume reduction greater than 15% of the baseline tumor size at follow-up showed early D changes, whereas ADC changes were not statistically significant.

Conclusion IVIM appears to be a useful tool for detecting early microstructural changes within meningiomas treated with proton therapy and may potentially be able to predict tumor response.

Keywords IVIM · Meningioma · DWI · Radiotherapy · Oncology

Introduction

Meningiomas represent the most common central nervous system primary neoplasm in the adult population [1, 2].

They appear as extra-axial masses, more frequently at the intracranial level, and, according to the World Health Organization (WHO) classification, can be subdivided into three histological grades with different levels of malignancy

Andrea Franconeri and Simone Sacco contributed equally to this work.

✉ Andrea Franconeri
afrancon88@gmail.com

1 Department of Clinical Surgical Diagnostic and Pediatric Sciences, University of Pavia, Pavia, Italy

2 UCSF Weill Institute for Neurosciences, Department of Neurology, University of California, San Francisco, CA, USA

3 Diagnostic Imaging Unit, National Center of Oncological Hadrontherapy (CNAO), Pavia, Italy

4 Neuroradiology Department, IRCCS Mondino Foundation, Pavia, Italy

5 Department of Electronics, Information and Bioengineering, Politecnico di Milano, Milan, Italy

6 Bioengineering Unit, National Center of Oncological Hadrontherapy (CNAO), Pavia, Italy

7 Radiotherapy Unit, National Center of Oncological Hadrontherapy (CNAO), Pavia, Italy

8 Radiology Institute, Fondazione IRCCS Policlinico San Matteo, Piazzale Golgi, Pavia, Italy

[2, 3]. Surgery is considered the gold standard treatment in most cases. However, in the case of incompletely excised, surgically inaccessible, recurrent, and higher grade meningiomas (WHO II and III), other treatment options can be considered, such as photon-based adjuvant fractionated radiotherapy, intensity-modulated radiotherapy (IMRT), volumetric modulated arc therapy (VMAT), and stereotactic radiotherapy [4]. More recently, particle therapy, either alone or within a mixed beam strategy, is being investigated in order to improve patients' outcome while reducing late toxicities by lowering scattered doses to adjacent normal tissue [4].

Magnetic resonance imaging (MRI) is the reference modality for the diagnosis and follow-up of meningiomas [5]. In the era of image-guided radiotherapy, MRI guarantees the best soft-tissue contrast as well as adequate functional information which allows for more precise radiation treatment delivery and dose escalation [6, 7]. Among functional techniques, diffusion-weighted imaging (DWI) assesses the Brownian motion of water molecules, allowing inferences based on specific microstructural features of neoplastic tissues, such as cell density.

Conventional DWI together with apparent diffusion coefficient (ADC) is widely used in radiotherapy [7]. In clinical practice, ADC is calculated using at least two b values (usually $b = 0$ and $b = 1000$ s/mm^2) through a mono-exponential diffusion model in which signal decay is influenced both by true molecular diffusion as well as by microvascular perfusion [8, 9]. Consequently, ADC values can be overestimated, especially in situations where microvascularity is increased because of tumor-specific histological features or radiation-induced inflammation.

More complex diffusion models, which further probe tissue microstructure and perfusion, have shown potential in radiotherapy. Intravoxel incoherent motion (IVIM) is a diffusion technique that utilizes multiple b values and a bi-exponential fitting to extrapolate the contribution of blood microcirculation in the capillary network from the global diffusion signal, defined as pseudo-diffusion (D*) [10]. The remnant signal is defined as true diffusion (D) and is thought to represent true water molecule diffusivity within tissues. The IVIM separate assessment of the two different diffusion signal decay components is of great interest. In fact, such assessment might provide relevant insights about the microstructural features of biological tissues [8, 11]. For this reason, IVIM may gain a role in the prediction of tumor histological grade [12–14].

However, another interesting IVIM application in the oncologic field is the use of a longitudinal approach for detecting underlying early treatment-related microvasculature and histological changes that is potentially able to predict the degree of final response to treatment such as chemotherapy or radiotherapy. In recent years, indeed, many studies have assessed the role of IVIM in predicting the therapeutic response of various neoplastic lesions and have witnessed promising results [15–27]. Among them, of particular interest is the potential role of early changes in IVIM parameters to predict response to treatments such as neoadjuvant chemotherapy in nasopharyngeal carcinoma and breast cancer [23, 25], and concurrent chemo-radiotherapy in advanced cervical cancers [24].

The purpose of our study is to provide a first longitudinal IVIM assessment of meningiomas treated with proton therapy to detect early microstructural changes that are potentially able to predict tumor response in the early phases of treatment.

Materials and methods

The present study was approved by the local IRB (The Ethics Committee, Pavia, Italy) and a detailed written informed consent form was signed by all subjects.

Subjects

Subjects with meningiomas, referred to our Center in preparation for proton therapy from January 2017 to July 2018, were retrospectively selected for participation in the present study. The inclusion criteria were the following: intracranial location of lesions, age over 18, and adequate quality of MRI scans for quantitative diffusion-weighted MR imaging assessment. Seventeen subjects (12 females, 5 males; mean age 57.9 ± 14.2 years) were eventually enrolled. Meningiomas were located on the skull base in 12 cases and at the convexity in 1 case, whereas 4 subjects showed multiple lesions consistent with meningiomatosis. In the latter cases, only the largest lesion was analyzed. Three meningiomas showed brain invasiveness and only one showed bone invasiveness. Ten out of 17 subjects underwent surgery at least 6 months before baseline MRI, whereas 4 out of 17 underwent conventional radiotherapy at least 12 months before baseline MRI. Overall, only 6 out of 17 subjects were not previously treated with surgery and/or radiotherapy.

MRIs protocol and imaging analysis

Subjects underwent baseline MRI before proton therapy treatment, as well as a follow-up examination at 6 months after the end of treatment. Two out of 17 subjects, however, could not undergo the follow-up MRI due to technical reasons. Proton therapy was administered in 30 fractions (1.8 Gy per fraction) for a total dose of 54 Gy. During treatment, all subjects underwent four additional MRI evaluations before the 1st treatment fraction (t0), immediately after the 10th (t10), 20th (t20), and the last fraction (t30) of proton-therapy.

All MRIs were performed on a 3T scanner (Magnetom Verio, Siemens, Germany) with a standard 32-channel head coil.

Baseline and follow-up (6 months) MRIs included the following sequences:

- Axial T1 Turbo Spin Echo (TSE), axial T2 TSE, axial T2 Gradient echo (GE), axial Fluid-attenuated inversion recovery (FLAIR).
- Echo-planar imaging two-dimensional (EP2D) DWI with seven b values equal to 0, 50, 100, 150, 200, 400, and 1000 s/mm^2; voxel size $1.9 \times 1.9 \times 4$ mm, phase encoding AP, TR/TE = 5800/75 ms, FA: 90°, field of view (FOV) = 247×300 mm; acquisition matrix = 160×132; number of averages = 3; and GRAPPA (Generalized Autocalibrating Partial Parallel Acquisition). The definition of the number of b values satisfied recommendations [24] reported for the computation of a simplified IVIM model. Specifically, the best time-quality trade-off was reached by acquiring scans with only two b values (400 and 1000 s/mm^2) in the $b > 200$ s/mm^2 regime [24], whereas b values in the 0.50 s/mm^2 interval were not achievable due to scanner limitations.
- Axial T1 Volumetric Interpolated Breath-hold Examination (VIBE) fat saturated with 0.6-mm isotropic voxel after injection of a gadolinium-based contrast agent (gadoteridol 0.2 mL/kg); voxel size $0.6 \times 0.6 \times 0.6$ mm, TR = 5.35 ms, TE = 2.27 ms, and FA: 11.5°.

The additional MRIs performed during treatment included only axial TSE T2-WI and DWI sequences, as described above.

ADC maps were computed through linear regression using all b values. IVIM parameters were derived from a nonlinear least square optimization; specifically, true diffusion (D), pseudo-diffusion (D*), and perfusion fraction (f) coefficient maps were computed voxel-wise by fitting the bi-exponential model: $S(b)/S(b=0) = (1-f) \cdot \exp(-b \cdot D) + f \cdot \exp(-b \cdot (D + D^*))$, where S(b) represents image intensities at b-values different from 0 and S (b = 0) is the image intensity of the diffusion image taken at b value 0 [10]. IVIM fitting was performed with an in-house software implemented in MATLAB. A bounded, trust-region, nonlinear least squares fit was used [14]. We did not use the 2-step procedure.

For all timepoints, meningiomas were manually segmented on axial T2 TSE in each single slide with the open-source software ITK-SNAP (www.itksnap.org). Since most of the subjects underwent biopsy and/or surgery before baseline, we evaluated GE sequences to exclude peripheral foci of magnetic susceptibility from baseline segmentations. In the case of bone invasiveness, the intraosseous part of meningiomas was not included in the ROI measurements.

The tumor contours were then rigidly registered (www.plastimatch.org) to DWI images taken at 0 s/mm^2 b value and acquired during the same session. All registration outputs were reviewed by 2 neuroradiologists with 10 and

8 years of experience in the field (L.F and A.B, respectively). We finally extracted, within the segmented lesions, tumor volumes as well as the median ADC, D, D*, and f values for all timepoints.

Statistical analysis

Statistical analysis was performed using the non-parametric Wilcoxon test at 95% confidence level ($\alpha = 0.05$). A population of 17 subjects was utilized for comparison of IVIM metrics and ADC values among intra-treatment timepoints, whereas a population of 15 subjects was utilized for assessing differences between baseline and follow-up as well as between intra-treatments timepoints and follow-up. Patients were further divided into two groups according to tumor volume changes between baseline and follow-up (threshold at 15%), and the two groups were then compared in terms of changes in diffusion parameters. Statistical analysis was performed with STATA v.15.1 (StataCorp USA 2017).

Results

Tumor volume changes over time

As shown in Fig. 1, tumor volume decreased from t0 to follow-up in 11 out of 15 subjects (mean change = $- 20.7 \pm 16.8\%$; range $- 62$ to $- 3.2\%$); however, only 7 out of 15 subjects showed a volume decrease greater than 15% of the baseline tumor volume (Fig. 2). Four out of 15 subjects showed increased tumor volume from baseline to follow-up (mean increase = $+ 19.7 \pm 9.7\%$; range $+ 31\%$ to $+ 7\%$).

ADC and IVIM metrics changes over time

No statistically significant baseline difference was detected in ADC and IVIM metrics among subjects previously treated with surgery and/or radiotherapy (11 out of 17) and subjects not previously treated (6 out of 17).

No statistically significant difference was detectable in ADC and IVIM metrics from baseline to t0. A progressive increase in ADC and D values was observed after t0 (Fig. 3) in addition to a progressive decrease in D* values (Fig. 4). In particular, statistically significant differences were found for ADC, D, and D* values between every timepoint and follow-up (Table 1).

No statistically significant changes in f values were detectable from t0 to follow-up.

Regarding intra-treatment timepoints, statistically significant early changes were detectable only for D values between t0 and t20 ($p = 0.03$) and t0 and t30 ($p = 0.02$) and ADC values between t0 and t20 ($p = 0.049$). Moreover, ADC values showed statistically significant changes from t10 to t20 ($p = 0.02$) and t10 to t30 ($p = 0.035$) (Table 2). No statistically

Fig. 1 Percentage of tumor volume changes between t0 and follow-up in 15 subjects. Only 7 subjects, highlighted in gray, showed a decrease in volume greater than 15% of the original tumor size (Group 1). Eight subjects, highlighted in black, showed a decrease of less than 15% of the original tumor size, or an increase in size at follow-up (Group 2)
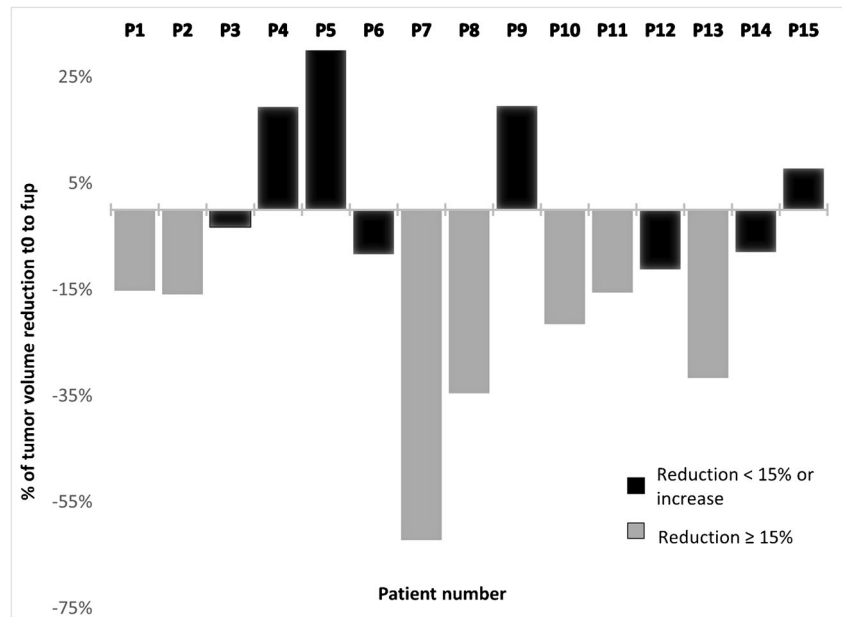
significant differences among intra-treatment timepoints were found for f or D* values.

Comparison of ADC and D values changes among subjects grouped by different volume changes from baseline to follow-up

Since early changes among intra-treatment timepoints were detectable only for D and ADC values, we decided to assess differences in these parameters among subjects grouped on the basis of tumor volume changes from baseline to follow-up (Fig. 1):

– Group 1: subjects showing a decrease greater than the 15% of their baseline volume ($n = 7$), suggesting a good response to treatment
– Group 2: subjects showing either an increase of their volume from baseline or a decrease of less than the 15% of their baseline volume ($n = 8$), suggesting a lack of response or only moderate response to treatment

Fig. 2 52-year-old female patient with a left parietal skull vault meningioma treated with proton-therapy. Axial TSE T2-weighted MRI sequences at different timepoints. Progressive decrease in volume from baseline (a) to follow-up (f) through intra-treatment timepoints (t0 b, t10 c, t20 d, t30 e)
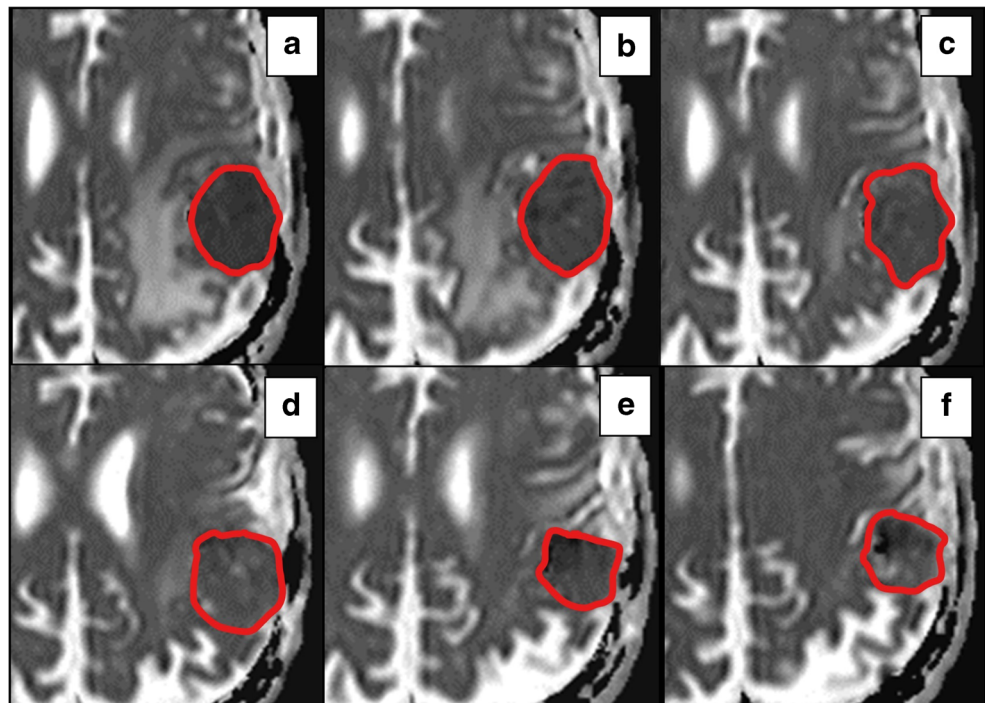
Table 1 *P*-values from the comparison between intra-treatment timepoints and follow-up of median values of different IVIM parameters

p values		t0	t10	t20	t30
ADC (median)	F-up	*0.009*	*0.001*	*0.006*	*0.019*
D (median)	F-up	*0.001*	*0.002*	*0.001*	*0.001*
D* (median)	F-up	*0.013*	*0.003*	*0.011*	*0.001*
f (median)	F-up	0.153	0.091	0.463	0.583

Statistically significant *p* values are highlighted in bold and italics ($\alpha = 0.05$)

Group 1 showed a statistically significant increase in D values from t0 to t20 ($p < 0.05$), whereas group 2 did not exhibit such a finding. Conversely, no ADC statistically significant changes were detectable in either group from t0 to t20. No D or ADC statistically significant differences were detectable among the 2 groups at baseline.

Discussion

The purpose of our study was to provide an intra-treatment longitudinal IVIM assessment of meningiomas treated with proton therapy to detect early microstructural changes potentially able to predict tumor response and drive and adapt treatment delivery.

Specifically, we detected statistically significant increases in both ADC and D values from baseline to early phases of treatment, but, unlike ADC, early changes in D values were particularly associated with greater tumor volume reduction. Indeed, subjects that had a reduction of tumor size at follow-up greater than 15% of the baseline values (Group 1) showed early D, but not early ADC changes.

The reason for this mismatch is probably connected to the intrinsically different nature of ADC and D. While ADC assesses the overall diffusion signal within a tissue, D represents the perfusion-free diffusion portion of ADC and is therefore a more specific parameter for assessing restricted water diffusion within cells [8, 28, 29]. D changes in early phases of treatment are likely to be specifically connected with a reduction in cell density [20], whereas ADC values might also have been influenced by subtle changes in blood perfusion due to radiation-induced tissue inflammation. In fact, even if D* showed a significant decrease in values from t0 to follow-up without statistically significant intra-treatment changes, we noticed fluctuations of this parameter when analyzing intra-treatment trends (Fig. 4). Specifically, we hypothesize that D* might fluctuate during radiotherapy treatments by showing increased values at first, possibly because of early radiation-related inflammatory changes, and successively showing a decrease over time, due to progressive post-treatment vessel degeneration.

Our study is in partial accordance with some previous works analyzing IVIM parameters as predictors of therapy response in several oncological diseases. At least 4 studies have shown that pre-treatment D values predicted response to therapy in nasopharyngeal carcinoma as well as in head and neck squamous cell carcinoma [15, 18, 23, 25]. In one of these analyses, there was a considerable increase in sensitivity when differences in D values before and after chemotherapy were considered [23]. These results are probably connected to the fact that highly cellular tumors, with lower baseline D values and rapidly dividing cells, are more sensitive to chemo- and radiotherapy and are therefore associated with a better prognosis [21]. Differently from these studies, our data did not show statistically significant differences in baseline D values between groups characterized by different volume changes over time, most likely due to the low number of subjects enrolled in the study which thus decreases statistical power. Nonetheless, the increases in D values detected during early phases of proton-therapy might represent a sign of good response to treatment.

Regarding other IVIM parameters assessing microcirculation, even though a good correlation between f values and histological vascular density has been reported in meningiomas [28], D* and f did not present statistically significant early changes within treated lesion. Although this might be

Fig. 3 Median ADC and D values over time between intra-treatment timepoints and follow-up: both ADC and D show a progressive increase in values starting from early intra-treatment timepoints
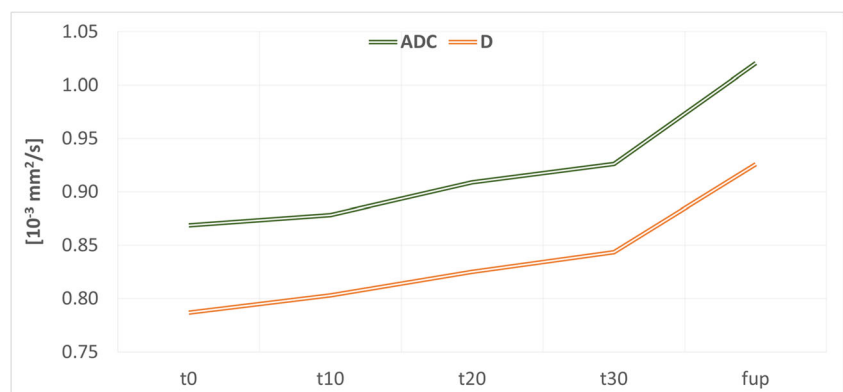
Fig. 4 Median pseudo-diffusion (D*) value changes over time between intra-treatment timepoints and follow-up: D* values show fluctuations in values among intra-treatment timepoints without any statistically significant changes. D* values show a statistically significant decrease at follow-up
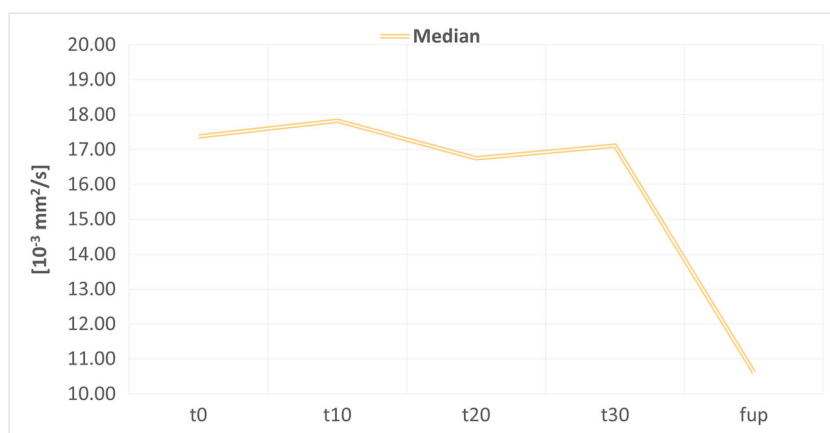
related to the small cohort of patients, it should be noted that fewer studies have reported the ability of these metrics to predict response, specifically two for f [18, 26] and one for D* [17].

Additionally, it should be noted that signal attenuation at low b values results from blood microcirculation effects (D* and f), while at very high b values, the signal depends on slow true diffusion movements (D) [11]. Therefore, the lack of DWI imaging with b values lower than 50 s/mm^2 in our study could have reduced the accuracy of perfusion-related parameters. Despite this, a simplified IVIM model can still provide clinically relevant information, as recently reported by Conklin and colleagues [30], where perfusion maps of conventional IVIM (using nonlinear fitting of the standard bi-exponential equation) were compared with those derived from a simplified IVIM model (using linear fitting of the log-normalized signal curves for subsets of b values > 200 s/mm^2) on 49 patients with gliomas and 17 with acute strokes [30]. In this study, reducing the number of b values in the computation of f resulted in lower accuracy and increased variability of the estimated perfusion fraction when compared with a full bi-exponential fitting approach, but the simplified IVIM approach was still able to detect clinically meaningful differences between high- and low-grade tumors and between ischemic and healthy brain tissues [30]. Based on these results, Conklin and colleagues suggested a minimum of 4 nonzero b values for the clinical application of simplified IVIM procedures, as performed in our study.

Our study presents several limitations. The first is represented by the limited number of subjects enrolled ($n = 17$), with only 15 presenting a follow-up MRI. The short follow-up observation period (6 months) represents another limit, particularly in the assessment of long-term therapeutic response. Therefore, our results need to be validated in larger cohorts. Another confounding factor is related to the enrollment of subjects who were previously treated with surgery and/or conventional radiotherapy, which was completed at least 12 months before baseline. Radiotherapy might induce changes within tissues, such as intralesional scarring, which may affect quantitative diffusion metrics. Nonetheless, it should be noted that certain parts of some tumors which were segmented at baseline had previously shown a progressive increase in size following the abovementioned therapies as a result of ineffective treatments. Furthermore, while the presence of hemosiderin caused by previous surgeries may have affected quantitative diffusion metrics, we think that the use of GE sequences as guides in avoiding areas of lower signal minimized the issue. Lastly, the lack of b values in the range of 0–50 s/mm^2 due to technical limitations may have reduced the accuracy of the IVIM perfusion-related parameters.

Future goals include collecting data on a larger cohort by both extending post-treatment follow-ups of already enrolled subjects, as well as enrolling new ones. Reanalyzing pre-treatment IVIM parameters and correlating D and ADC values with histological patterns might allow a better assessment and definition of the different prognostic factors in the therapeutic response.

Table 2 p values from the comparison among intra-treatment timepoints of D and ADC median values

		t0	t10	t20	t30			t0	t10	t20	t30
D (median)	t0					**ADC (median)**	t0				
	t10	*0.078*					t10	*0.491*			
	t20	***0.030***	*0.091*				t20	***0.049***	***0.020***		
	t30	***0.020***	*0.153*	*0.173*			t30	*0.119*	***0.035***	*0.358*	

Statistically significant p values are highlighted in bold and italics ($\alpha = 0.05$)

Conclusion

We have shown the potential role of IVIM parameters in assessing early changes within meningiomas treated with proton therapy. The early detection of subjects who are destined to benefit less from the treatment could be highly beneficial in adjusting the radiation dose, thus increasing the chance of an optimal response. Additionally, the early detection of specific areas within meningiomas that are more likely to show a worse response might allow for tailored corrections of radiotherapy treatments.

Compliance with ethical standards

Conflict of interest   The authors declare that they have no conflict of interest.

Ethical approval   All procedures performed in the studies involving human participants were in accordance with the ethical standards of the institutional and/or national research committee and with the 1964 Helsinki Declaration and its later amendments or comparable ethical standards.

Informed consent   Informed consent was obtained from all individual participants included in the study.

References

1. Whittle IR, Smith C, Navoo P, Collie D (2004) Meningiomas. Lancet Lond Engl 363(9420):1535–1543
2. Barresi V, Caffo M, Tuccari G (2016) Classification of human meningiomas: lights, shadows, and future perspectives. J Neurosci Res 94(12):1604–1612
3. Louis DN, Perry A, Reifenberger G, von Deimling A, Figarella-Branger D, Cavenee WK, Ohgaki H, Wiestler OD, Kleihues P, Ellison DW (2016) The 2016 World Health Organization classification of tumors of the central nervous system: a summary. Acta Neuropathol (Berl) 131(6):803–820
4. Brastianos PK, Galanis E, Butowski N, Chan JW, Dunn IF, Goldbrunner R, Herold-Mende C, Ippen FM, Mawrin C, McDermott MW, Sloan A, Snyder J, Tabatabai G, Tatagiba M, Tonn JC, Wen PY, Aldape K, Nassiri F, Zadeh G, Jenkinson MD, Raleigh DR, International Consortium on Meningiomas, Aldape K, Au K, Barnhartz-Sloan J, Bi WL, Brastianos PK, Butowski N, Carlotti C, Cusimano MD, DiMeco F, Drummond K, Dunn IF, Galanis E, Giannini C, Goldbrunner R, Griffith B, Hashizume R, Hanemann CO, Herold-Mende C, Horbinski C, Huang RY, James D, Jenkinson MD, Jungk C, Kaufman TJ, Krischek B, Lachance D, Lafougère C, Lee I, Liu JC, Mamatjan Y, Mansouri A, Mawrin C, McDermott M, Munoz D, Nassiri F, Noushmehr H, Ng HK, Perry A, Pirouzmand F, Poisson LM, Pollo B, Raleigh D, Sahm F, Saladino A, Santarius T, Schichor C, Schultz D, Schmidt NO, Selman W, Sloan A, Spears J, Snyder J, Suppiah S, Tabatabai G, Tatagiba M, Tirapelli D, Tonn JC, Tsang D, Vogelbaum MA, Deimling A, Wen PY, Walbert T, Westphal M, Workewych AM, Zadeh G (2019) Advances in multidisciplinary therapy for meningiomas. Neuro-Oncology 21(Suppl 1):i18–i31. https://doi.org/10.1093/neuonc/noy136
5. Buerki RA, Horbinski CM, Kruser T, Horowitz PM, James CD, Lukas RV (2018) An overview of meningiomas. Future Oncol Lond Engl 14(21):2161–2177
6. Jaffray DA (2012) Image-guided radiotherapy: from current concept to future perspectives. Nat Rev Clin Oncol 9(12):688–699. https://doi.org/10.1038/nrclinonc.2012.194
7. Gurney-Champion OJ, Mahmood F, van Schie M, Julian R, George B, Philippens MEP, van der Heide UA, Thorwarth D, Redalen KR (2020) Quantitative imaging for radiotherapy purposes. Radiother Oncol 146:66–75
8. Le Bihan D, Breton E, Lallemand D, Aubin ML, Vignaud J, Laval-Jeantet M (1988) Separation of diffusion and perfusion in intravoxel incoherent motion MR imaging. Radiology 168(2):497–505
9. Le Bihan D, Breton E, Lallemand D, Grenier P, Cabanis E, Laval-Jeantet M (1986) MR imaging of intravoxel incoherent motions: application to diffusion and perfusion in neurologic disorders. Radiology 161(2):401–407
10. Le Bihan D (2019) What can we see with IVIM MRI? Neuroimage 187:56–67. https://doi.org/10.1016/j.neuroimage.2017.12.062
11. Iima M, Le Bihan D (2016) Clinical intravoxel incoherent motion and diffusion MR imaging: past, present, and future. Radiology 278(1):13–32
12. Sacco S, Ballati F, Gaetani C, Lomoro P, Farina LM, Bacila A, Imparato S, Paganelli C, Buizza G, Iannalfi A, Baroni G, Valvo F, Bastianello S, Preda L (2020) Multi-parametric qualitative and quantitative MRI assessment as predictor of histological grading in previously treated meningiomas. Neuroradiology 62(11):1441–1449
13. Bohara M, Nakajo M, Kamimura K, Yoneyama T, Fukukura Y, Kiyao Y, Yonezawa H, Higa N, Kirishima M, Yoshiura T (2020) Histological grade of meningioma: prediction by intravoxel incoherent motion histogram parameters. Acad Radiol 27(3):342–353
14. Zampini MA, Buizza G, Paganelli C, Fontana G, D'Ippolito E, Valvo F, Preda L, Baroni G (2020) Perfusion and diffusion in meningioma tumors: a preliminary multiparametric analysis with dynamic susceptibility contrast and intravoxel incoherent motion MRI. Magn Reson Imaging 67:69–78
15. Ding Y, Hazle JD, Mohamed ASR, Frank SJ, Hobbs BP, Colen RR, Gunn GB, Wang J, Kalpathy-Cramer J, Garden AS, Lai SY, Rosenthal DI, Fuller CD (2015) Intravoxel incoherent motion imaging kinetics during chemoradiotherapy for human papillomavirus-associated squamous cell carcinoma of the oropharynx: preliminary results from a prospective pilot study. NMR Biomed 28(12):1645–1654
16. Granata V, Fusco R, Catalano O, Filice S, Amato DM, Nasti G, Avallone A, Izzo F, Petrillo A (2015) Early assessment of colorectal cancer patients with liver metastases treated with antiangiogenic drugs: the role of intravoxel incoherent motion in diffusion-weighted imaging. PLoS One 10(11):e0142876
17. Guo W, Luo D, Lin M, Wu B, Li L, Zhao Y, Yang L, Zhou C (2016) Pretreatment intra-voxel incoherent motion diffusion-weighted imaging (IVIM-DWI) in predicting induction chemotherapy response in locally advanced hypopharyngeal carcinoma. Medicine (Baltimore) 95(10):e3039
18. Hauser T, Essig M, Jensen A, Laun FB, Münter M, Maier-Hein KH, Stieltjes B (2014) Prediction of treatment response in head and neck carcinomas using IVIM-DWI: evaluation of lymph node metastasis. Eur J Radiol 83(5):783–787
19. Hou J, Yu X, Hu Y, Li F, Xiang W, Wang L, Wang H, Lu Q, Zhang Z, Zeng W (2016) Value of intravoxel incoherent motion and dynamic contrast-enhanced MRI for predicting the early and short-term responses to chemoradiotherapy in nasopharyngeal carcinoma. Medicine (Baltimore) 95(35):e4320
20. Marzi S, Piludu F, Sanguineti G, Marucci L, Farneti A, Terrenato I, Pellini R, Benevolo M, Covello R, Vidiri A (2017) The prediction of the treatment response of cervical nodes using intravoxel incoherent motion diffusion-weighted imaging. Eur J Radiol 92:93–102

21. Noij DP, Martens RM, Marcus JT, de Bree R, Leemans CR, Castelijns JA, de Jong MC, de Graaf P (2017) Intravoxel incoherent motion magnetic resonance imaging in head and neck cancer: a systematic review of the diagnostic and prognostic value. Oral Oncol 68:81–91

22. Park YS, Lee CH, Kim JH, Kim IS, Kiefer B, Seo TS, Kim KA, Park CM (2014) Using intravoxel incoherent motion (IVIM) MR imaging to predict lipiodol uptake in patients with hepatocellular carcinoma following transcatheter arterial chemoembolization: a preliminary result. Magn Reson Imaging 32(6):638–646

23. Xiao Y, Pan J, Chen Y, Chen Y, He Z, Zheng X (2015) Intravoxel incoherent motion-magnetic resonance imaging as an early predictor of treatment response to neoadjuvant chemotherapy in locoregionally advanced nasopharyngeal carcinoma. Medicine (Baltimore) 94(24):e973

24. Zhu L, Wang H, Zhu L, Meng J, Xu Y, Liu B, Chen W, He J, Zhou Z, Yang X (2017) Predictive and prognostic value of intravoxel incoherent motion (IVIM) MR imaging in patients with advanced cervical cancers undergoing concurrent chemo-radiotherapy. Sci Rep 7(1):11635

25. Cho GY, Gennaro L, Sutton EJ, et al. Intravoxel incoherent motion (IVIM) histogram biomarkers for prediction of neoadjuvant treatment response in breast cancer patients. - PubMed - NCBI. https://www.ncbi.nlm.nih.gov/pubmed/28856177. Accessed October 5, 2019

26. Lee YJ, Kim SH, Kang BJ, et al. Intravoxel incoherent motion (IVIM)-derived parameters in diffusion-weighted MRI: Associations with prognostic factors in invasive ductal carcinoma. - PubMed - NCBI. https://www.ncbi.nlm.nih.gov/pubmed/27796081. Accessed October 5, 2019

27. Sun H, Xu Y, Song A, Shi K, Wang W. Intravoxel incoherent motion MRI of rectal cancer: correlation of diffusion and perfusion characteristics with prognostic tumor markers. - PubMed - NCBI. https://www.ncbi.nlm.nih.gov/pubmed/29446674. Accessed October 5, 2019

28. Togao O, Hiwatashi A, Yamashita K, Kikuchi K, Momosaka D, Yoshimoto K, Kuga D, Mizoguchi M, Suzuki SO, Iwaki T, Van Cauteren M, Iihara K, Honda H (2018) Measurement of the perfusion fraction in brain tumors with intravoxel incoherent motion MR imaging: validation with histopathological vascular density in meningiomas. Br J Radiol 91(1085):20170912

29. Togao O, Hiwatashi A, Yamashita K, Kikuchi K, Mizoguchi M, Yoshimoto K, Suzuki SO, Iwaki T, Obara M, Van Cauteren M, Honda H (2016) Differentiation of high-grade and low-grade diffuse gliomas by intravoxel incoherent motion MR imaging. Neuro-Oncology 18(1):132–141

30. Conklin J, Heyn C, Roux M, Cerny M, Wintermark M, Federau C (2016) A simplified model for intravoxel incoherent motion perfusion imaging of the brain. AJNR 37(12):2251–2257